NASA TECHNICAL MEMORANDUM

NASA TM X-52794

NASA TM X-52794

FRACTURE OF THIN SECTIONS CONTAINING THROUGH AND PART-THROUGH CRACKS

by Thomas W. Orange, Timothy L. Sullivan, and Frederick D. Calfo
Lewis Research Center
Cleveland, Ohio

TECHNICAL PAPER proposed for presentation at
Symposium on Fracture Toughness Testing at Cryogenic Temperatures
sponsored by the American Society for Testing and Materials
Toronto, Canada, June 22-26, 1970

FRACTURE OF THIN SECTIONS CONTAINING THROUGH AND PART-THROUGH CRACKS

by Thomas W. Orange, Timothy L. Sullivan, and Frederick D. Calfe

Lewis Research Center
Cleveland, Ohio

TECHNICAL PAPER proposed for presentation at
Symposium on Fracture Toughness Testing at Cryogenic Temperatures sponsored by the American Society for Testing and Materials
Toronto, Canada, June 22-26, 1970

NATIONAL AERONAUTICS AND SPACE ADMINISTRATION

ABSTRACT: Current fracture mechanics theory is used to illustrate the effects of crack dimensions and material properties on fracture stresses for through-thickness and part-through cracks. The implications of the analysis for leak-before-burst design of pressure vessels are discussed.

The applicability of plane-strain theory to surface cracks in thin metal sections was studied experimentally. Specimens containing surface cracks of various depths and lengths and specimens with through cracks in the same range of crack lengths were tested. Titanium-5Al-2.5SN-ELI (0.06- and 0.11-in. (1.6- and 2.9-mm) thick) were tested at -423 F (20 K); the 2219-T87 alloy was also tested at +70 and -320 F (300 and 77 K).

The fracture tests indicate that when Irwin's plastic zone size was less than about one-tenth of the uncracked ligament depth (thickness minus crack depth), surface-crack fracture behavior was in agreement with plane-strain theory. When the plastic zone was greater than the ligament depth, fracture stresses for surface-crack specimens were very nearly the same as for specimens with through-cracks of the same original length.

KEY WORDS: fracture mechanics, fracture strength, part-through cracks, aluminum alloys, and titanium alloys.

Fracture of Thin Sections Containing Through and Part-Through Cracks

by Thomas W. Orange, Timothy L. Sullivan, and Frederick D. Calfo

Summary

This paper presents the results of an investigation of the applicability of plane-strain fracture mechanics theory to problems of surface cracks in thin metal sections. Fracture mechanics analysis is used to illustrate the effects of crack dimensions and material properties on fracture stress for through and part-through cracks. The currently-accepted limits for the validity of the analyses are reviewed. Experimental results and the limitations they impose on the applicability of the analysis are discussed.

Included are the results of thin-sheet fracture tests of several materials at ambient and cryogenic temperatures. The materials and test temperatures are:

Titanium-5Al-2.5Sn-ELI, 0.06- and 0.11-in. (1.6- and and 2.9-mm) thick at -423 F (20 K)

Aluminum 2014-T6, 0.06-in. (1.6-mm) thick, at -423 F (20 K)

Aluminum 2219-T87, 0.07-in. (1.6-mm) thick, at +70, -320, and -423 F (300, 77, and 20 K).

Specimens containing semi-elliptical surface cracks of various lengths and depths and specimens containing through-thickness cracks in the same range of crack lengths were tested. The results are examined in the light of current fracture mechanics theory.

Introduction

Linear elastic fracture mechanics can be used with confidence only for a limited number of practical crack problems at the present time. Some of the uncertainties associated with through-crack testing are mentioned in [1] (authors' reply to discussion by R. H. Heyer). Irwin's surface-crack fracture analysis [2] assumes that conditions of plane strain prevail, and its application is customarily limited to crack depths less than half the plate thickness. However, in spite of these apparently severe limitations, fracture mechanics theory is still useful. It can provide at least a qualitative description of the effects of material and geometrical parameters on fracture strength. In some cases, as will be shown later, it can also give a good quantitative description.

Current fracture mechanics analysis is based on linear elastic theory. In lieu of an elasto-plastic analysis, non-brittle materials are treated in an approximate manner. Localized yielding at the tip of a crack is accounted for by adding a portion of the plastic zone length to the actual crack length. As long as the plastic zone is small compared to the crack length and specimen dimensions, this approximation has proven useful.

For small-scale yielding, the plastic zone size is proportional to the square of the ratio of stress intensity to yield strength. Thus simple plastic zone corrections should be adequate as long as the crack length and specimen dimensions are greater than some multiple of this ratio squared. For edge-cracked or through-cracked specimens, the significant specimen dimensions are considered to be the crack length,

uncracked ligament length, and thickness. The proposed American Society for Testing and Materials (ASTM) plane-strain toughness test method [3] requires that thickness and crack length be greater than $2.5(K_{Ic}/\sigma_{ys})^2$, and implies that the ligament length (width minus crack length) be greater than about $2(K_{Ic}/\sigma_{ys})^2$. These criteria should be sufficiently conservative as to apply to all classes of materials. However, for some materials and/or test specimens (for example, [4]) the theory appears applicable (within engineering accuracy) to much smaller cracks as well.

Irwin's analysis for a surface crack in a plate [2] assumes that plane strain conditions prevail at fracture and that the crack dimensions are small compared with the plate dimensions. Brown and Srawley ([1], pp. 30-33) indicate that the analysis may not be applicable if the crack depth is less than $2.5(K_{Ic}/\sigma_{ys})^2$. Although the concept has not been adequately tested, there should probably be a minimum ligament depth (in this case, plate thickness minus crack depth) requirement also, as there is for the edge-crack specimens. Thus, for two reasons (depth-to-thickness limit and minimum ligament depth), application of the analysis to material thicknesses much less than $5(K_{Ic}/\sigma_{ys})^2$ cannot be assured.

The analysis of through cracks under mixed-mode failure conditions is also uncertain. It is well known that K_c decreases with increasing thickness until it reaches the limiting plane-strain value K_{Ic}. As discussed in [5] (pp. 138-143 and 155-158), K_c is not necessarily independent of crack length and specimen width. However, for many

materials the form of the crack-extension resistance curve (R-curve) is such that, for sufficiently large test specimens, K_c is essentially constant (for example, [6]). It is also possible to compute a nominal toughness parameter K_{cn} based on final load and original crack length (neglecting subcritical crack growth), but this is less likely to be constant. Although it is unsuitable for component design purposes, as shown by Kuhn [7], the concept of a constant K_{cn} is useful for the illustrative examples to follow.

The plastic zone at the crack tip is even less well understood than the subjects just discussed. Different analytical models lead to significantly different estimates of both the size and shape of the plastic zone. When used as corrections to a large crack length, these discrepancies will affect fracture toughness calculations only slightly. But uncertainty regarding the plastic zone size makes it very difficult to predict whether or not the plastic zone at the tip of a surface crack will extend completely through the plate thickness prior to failure. As will be shown later, this appears to significantly affect fracture behavior.

Rice has discussed various analytical models at length in [8]. Hahn and Rosenfield [9] have compared observed plastic zones in Fe-3Si steel with several analytical models. They conclude that none of the models completely described the observed plastic zones, which were somewhat "butterfly-shaped." Lacking an exact description, a lower bound on the plastic zone size is still possible. The results of [9] suggest that the extent of the plastic zone (projected onto the crack plane)

is roughly twice Irwin's plastic zone size term of [2], in the absence of large-scale yielding and nearby stress-free surfaces. Thus if the uncracked ligament behind a surface crack is less than twice Irwin's plastic zone size, one can be almost certain that the plastic zone has actually spread completely through the thickness. Note that if the plastic zone at the tip of a crack is "butterfly-shaped," it might (under rising load) first reach the back surface at points out of the crack plane, as in Fig. 1 (taken from [10]).

In the present paper, fracture mechanics analysis is used to predict the effects of crack dimensions and material properties on fracture stress for through cracks and part-through surface cracks. Fracture specimens with through cracks and with surface cracks were tested at cryogenic temperatures. The results are compared with the predicted trends.

Symbols

a	depth of semi-elliptical surface crack
c	half-length of through crack or semi-elliptical surface crack
K_c	fracture toughness under mixed-mode fracture conditions
K_{cn}	nominal value of K_c, based on original crack length and final load
K_{Ic}	opening-mode (plane-strain) fracture toughness
K_Q	apparent value of K_{Ic}
M	free-surface correction factor (magnification factor)
t	plate thickness
Φ	complete elliptical integral of the second kind for the argument $k^2 = 1 - a^2/c^2$

σ fracture stress (based on gross area)

σ_{ys} material yield strength (0.2 percent offset)

Analysis

Effects of Crack Geometry

Even though its application to design problems is somewhat restricted, current fracture mechanics theory can be used to illustrate the effects of crack geometry and material properties on fracture strength and fracture behavior. For the sake of discussion, assume that through cracks are governed by plane-stress conditions and surface cracks by plane-strain.

Fracture stresses for through-thickness cracks (from [1]) and for surface cracks (from [2]) in a wide flat plate can be written as

$$\sigma_{thru} = K_c \div \sqrt{\frac{\pi}{2} 2c + \frac{1}{2}\left(\frac{K_c}{\sigma_{ys}}\right)^2} \tag{1a}$$

$$\sigma_{surf} = K_{Ic} \div \frac{M}{\Phi} \sqrt{\pi a + \frac{1}{4\sqrt{2}}\left(\frac{K_{Ic}}{\sigma_{ys}}\right)^2} \tag{1b}$$

where Φ is a function of crack shape and M is a free-surface correction factor (taken by Irwin to be ~1.1 for crack depths less than half thickness). The correction factor of Kobayashi and Moss (denoted as M_e in [11]) was used (rather than Irwin's) so that cracks deeper than half thickness might be considered in this paper. For the reader's convenience, a plot of M/Φ is included as Fig. 2.

For purposes of illustration, it is appropriate (as discussed by Irwin

and Srawley in [12]) to consider the case where $t = K_c^2/2\pi\sigma_{ys}^2$. The previous equations can then be written as

$$\frac{\sigma_{thru}}{\sigma_{ys}} = \sqrt{2}\left(\frac{1}{2}\frac{2c}{t} + 1\right)^{-1/2} \tag{2a}$$

$$\frac{\sigma_{surf}}{\sigma_{ys}} = \sqrt{2}\,\frac{K_{Ic}}{K_c}\,\frac{\Phi}{M}\left[\frac{a}{t} + \frac{1}{2\sqrt{2}}\left(\frac{K_{Ic}}{K_c}\right)^2\right]^{-1/2} \tag{2b}$$

These equations are plotted in Fig. 3 for the case where $K_{Ic} = 0.5\,K_c$. Eq. (2b) is plotted for constant crack shape (a/2c) as well as for constant depth (a/t). The largest depth plotted is that for which the plastic zone is expected to just extend completely through the plate thickness at fracture. The applicability of the analysis to deeper cracks is highly questionable. If, as discussed earlier, the actual plastic zone size is taken to be twice Irwin's term, the limiting depth is

$$\left(\frac{a}{t}\right)_{max} = 1 - \frac{1}{\sqrt{2}}\left(\frac{K_{Ic}}{K_c}\right)^2 \tag{3}$$

Fig. 3 shows that theoretically a surface crack can fracture (or at least start to fracture) at a lower stress than a through crack of the same length, and that this would be most likely to occur for a deep crack with a/2c about 0.2 to 0.3. With the aid of Fig. 2 we can speculate on the effect of crack geometry on the actual fracture process. Consider a surface crack whose geometry is defined by the point "A." When the

load is increased to 0.8 σ_{ys}, the crack should start to propagate rapidly through the thickness with little if any increase in crack length. But the stress required to propagate a through crack of the same length is much greater (about 0.9 σ_{ys}). Thus the crack should self-arrest and become a stable through-thickness crack. If the crack were in a pressure vessel, the vessel would leak rather than fail catastrophically.

Consider now a surface crack whose geometry is defined by the point "B." When the load is increased to 0.7 σ_{ys}, the crack should start to propagate through the thickness. But if there is no load relaxation, the applied stress will be more than sufficient to propagate a through crack of that length and the crack should continue to propagate. A pressure vessel with such a crack would probably fail catastrophically (burst).

For the surface crack defined by point "C," the plastic zone would surely grow through the thickness prior to failure, and most of the uncracked ligament would undergo plastic deformation. Under these conditions, fracture might well be controlled by the stress intensity at or near the major axis of the semi-ellipse. If this crack were in a pressure vessel, elastic theory cannot predict whether it would leak or burst. Lacking more powerful analytical methods, we might speculate that if the crack opening displacement were sufficiently large the ligament might fail by tensile instability (and the vessel would leak), and that this would be most likely for long cracks. But the yielded ligament might also act as a plastic hinge, allowing the cracked region to bulge outward in the manner associated with through cracks [13]. This would induce a bending stress which would further complicate the problem. Under these conditions it would be

unwise to expect a cracked tensile specimen to simulate the behavior of a cracked pressure vessel.

The empirical relation developed by Eiber et al. ([14], Fig. 15) for part-through vee-notches in gas line pipe is quite similar in appearance to Fig. 3 of this paper. Their burst tests also indicate that failure type (i.e., leak or burst) can be correlated with relative fracture stresses for through cracks and surface cracks of the same length. If fracture stress for a given surface crack is less than for a through crack of the same length, that surface crack will result in a leak at failure; if greater, catastrophic fracture will occur.

Effects of Material Properties

The limits of applicability of this analysis are also affected by the material properties. Eq. (3) shows that the limiting crack depth (at which the plastic zone just penetrates the thickness) is also a function of the ratio K_{Ic}/K_c. Fig. 4 shows the effect of K_{Ic}/K_c at the limiting depth (for this specific thickness). From this figure it appears that leak-before-burst failures cannot be predicted at all if K_{Ic} is greater than about 0.6 K_c (for this thickness), and they can be expected over a wider range of crack lengths if K_{Ic}/K_c is low. Again, a crack with a depth-to-length ratio (a/2c) of about 0.25 appears most likely to leak rather than burst at failure.

Experimental Procedure

Materials

The titanium alloy was purchased in two thicknesses rolled from the same heat. Mill analyses for both are given in Table 1. The 2014-T6 aluminum alloy (unclad) was from the same lot as used in an earlier study

[6]. The analysis given was made by a commercial laboratory. The 2219-T87 aluminum alloy (also unclad) was from the same lot studied in [15], and its analysis is also given in Table 1.

The tensile properties listed in Table 2 were determined using the standard tensile specimen shown in Fig. 5(a) with differential-transformer extensometers.

Fracture Specimens

Titanium fracture specimen configurations were as shown in Figs. 5(b) to 5(d). All 2014-T6 specimens were as shown in Fig. 5(d). The 2219-T87 specimens were sized per Figs. 5(e) and 5(f) to be directly comparable with the surface-crack specimens tested in [15].

Natural cracks were grown from crack-starters by low-stress fatigue cycling the specimens. Crack starters for all through-crack and most surface-crack specimens were made by electrical-discharge machining. For a few of the 2014-T6 surface-crack specimens, sharp surface grooves were machine-scribed. All through-crack and some surface-crack specimens were fatigue sharpened in tension. To obtain more elongated cracks, some surface cracks were extended in cyclic unidirectional bending. For all specimens, the nominal net cyclic stress was less than half the material yield strength.

Apparatus and Procedure

The 2219-T87 through-crack fracture specimens were fitted with anti-buckling guides and tested in a 400,000-lb- (1.8-MN-) capacity screw-powered tensile testing machine. All other specimens were tested in hydraulic machines having capacities of 20,000, 24,000, and 120,000 lb (89,

107, and 535 KN). For smooth tensile tests, differential-transformer extensometers were used to measure average strain over a 2-in. (5-cm) gage length. Cryogenic test temperatures were established by immersing the specimen in liquid nitrogen or liquid hydrogen. A vacuum-jacketed cryostat with multilayer insulation was used to minimize boiloff. Cryogenic liquid level was maintained several inches above the upper specimen grip, and carbon resistors were used as level sensors.

Results and Discussion

Nominal fracture toughness values for through-crack specimens were computed using the finite-width correction factor proposed by Feddersen ([1], pp. 77-79). Eq. (1(a)) can then be written

$$K_{cn} = \sigma\sqrt{W\theta \sec \theta} \quad \text{where} \quad \theta = \frac{\pi}{2}\left(\frac{2c}{W}\right) + \frac{1}{2W}\left(\frac{K_{cn}}{\sigma_{ys}}\right)^2 \tag{4}$$

Apparent fracture toughness (K_Q) values for surface-crack specimens were computed using Eq. (1(b)) (rearranged) and the free-surface correction factor of [11]. Fracture test results and some calculated quantities are listed in Tables 3 and 4.

Titanium Alloy

Fig. 6 presents fracture stresses for through cracks and surface cracks in the thinner (0.06-in.) titanium sheet at -423 F (20 K). The surface-crack tests are grouped according to depth-to-thickness ratio. The experimental trends are generally in good agreement with the predicted trends of Fig. 3. Nominal fracture toughness (K_{cn}) for the through-crack specimens was essentially constant [62 ksi$\sqrt{\text{in.}}$ (68 MNm$^{-3/2}$), av].

Apparent fracture toughness K_Q for the surface-crack tests was reasonably constant [47 ksi$\sqrt{\text{in.}}$ (52 MNm$^{-3/2}$), av] for all but the seven with cracks deeper than 70 percent of the thickness. Note (Fig. 6) that for the five of these with short cracks (2c ~0.18 in.), fracture stresses are within the scatter band for through-crack tests. Using the average K_Q value (47 ksi$\sqrt{\text{in.}}$), Irwin's plastic zone size is between 14 and 29 percent of the uncracked ligament depth for the seven deviant tests. However, as discussed earlier, this expression is probably a conservataive (low) estimate of the actual plastic zone size, which may be several times larger.

Fig. 7 presents fracture stresses for through cracks and surface cracks in the thicker (0.11-in.) titanium sheet, also at -423 F (20 K). Here the surface-crack shapes were essentially constant (a/2c = 0.3, approx.) as crack depth was varied. Nominal fracture toughness (K_{cn}) for through-crack specimens was essentially constant [83 ksi$\sqrt{\text{in.}}$ (91 MNm$^{-3/2}$), av], as was apparent toughness K_Q for surface-crack specimens [59 ksi$\sqrt{\text{in.}}$ (65 MNm$^{-3/2}$), av]. Note that fracture stresses for the three deepest surface-crack tests lie within or very near the scatter band for through-crack tests. For these three specimens, Irwin's plastic zone size (K_Q = 59 ksi$\sqrt{\text{in.}}$) is between 13 and 40 percent of the uncracked ligament depth.

Even though both thicknesses are from the same heat, the K_Q and K_{cn} average values are about 13 percent higher (and strengths are lower) for the thicker gage. However, the K_Q average values for both are within the range of K_{Ic} values reported in [16] for much thicker specimens.

Aluminum Alloys

Fig. 8 presents fracture stresses for through cracks and surface cracks in 2014-T6 aluminum sheet [0.06-in. (1.6-mm) thick] at -423 F (20 K). Note that only for the shortest cracks is there any apparent difference between fracture stresses for through cracks and for surface cracks. Nominal fracture toughness (K_{cn}) was approximately constant [52 ksi$\sqrt{\text{in.}}$ (57 MNm$^{-3/2}$), av] for all but the two shortest through cracks. Apparent toughness K_Q was also constant [26 ksi$\sqrt{\text{in.}}$ (28 MNm$^{-3/2}$), av] for all but the four deepest surface cracks. For these four, Irwin's plastic zone size (based on 26 ksi$\sqrt{\text{in.}}$) was deeper than any uncracked ligament. For the eight other specimens, Irwin's plastic zone size was between 26 and 72 percent of the depth of the uncracked ligaments. However, even though constant, the K_Q values are unusually low. The surface-crack K_Q values reported in [17] for 2014-T62 alloy 0.5-in. (13-mm) thick are nearly twice as large. If based on [17] values, Irwin's plastic zone would be deeper than any uncracked ligament. Analysis according to [11], where plastic zone size is related to fracture stress rather than stress intensity, also indicates that the plastic zone did extend completely through the thickness prior to fracture for every test.

Fig. 9 presents fracture stresses for through cracks and surface cracks in 2219-T87 aluminum sheet [0.07-in. (1.7-mm) thick] at ambient temperature, -320, and -423 F (300, 77, and 20 K). The surface-crack data are taken from [15]; through-crack specimens from the same lot of material were tested at the Lewis Research Center. Neither nominal

toughness (K_{cn}) nor apparent toughness K_Q were constant at any temperature, and the curves of Fig. 9 were simply drawn through the through-crack data. Note that again there is little difference in fracture stresses for surface cracks and for through cracks of the same length. Based on the estimated K_{Ic} values of [14] [47 ksi$\sqrt{\text{in.}}$ at 70, 50 ksi$\sqrt{\text{in.}}$ at -320 and -423 F (52 MNm$^{-3/2}$ at 300, 55 MNm$^{-3/2}$ at 77 and 20 K)] the Irwin plastic zone sizes were greater than all uncracked ligaments. Thus it is fairly certain that the surface crack plastic zones penetrated the thickness prior to fracture in every test.

Discussion of Results

The constant-K_{cn} concept is not sufficient to characterize through-crack fracture in the relatively tough 2219-T87 alloy. But for the less-tough titanium and 2014-T6 aluminum alloys, it relates fracture stress to original crack length quite well over the range of these tests.

The characterization of surface-crack fracture is not as straightforward. However, the results are consistent if they are classified according to the relative depths of the plastic zone and the uncracked ligament. For most of the titanium specimens, where Irwin's plastic zone size was less than about 13 percent of the uncracked ligament depth, K_Q values were essentially constant and the plane-strain model (Eq. (1(b)) seems appropriate. For all the aluminum specimens, the plastic zone is believed to have extended completely through the thickness. Here fracture appears to be strongly related to crack length and the mixed-mode fracture toughness (K_{cn}). The behavior of the remainder of the titanium specimens is harder to classify, but this may be due to the approximate nature of the plastic zone size term.

As discussed earlier, Irwin's surface-crack analysis should be usable if the actual plastic zone size is "small" with respect to the depth of the uncracked ligament. These tests suggest an approximate limit. If Irwin's plastic zone term is less than about one-tenth the depth of the uncracked ligament, the plane-strain model appears to be applicable even for thin sections. However, the parameter K_Q (which may or may not be equal to the plane-strain toughness K_{Ic}) must be carefully determined. When the plastic zone is greater than the depth of the uncracked ligament, final fracture usually appears to be related to crack length and mixed-mode fracture toughness.

The analysis and the preceeding discussion assume that surface cracks do not propagate until rapid fracture occurs. However, some investigators have recently observed stable subcritical growth of surface cracks in some materials. Just prior to fracture, such a crack could be larger than its original dimensions but not yet through the thickness. In such a case, a K_Q value based on original crack depth and maximum load would be erroneously low. Subcritical growth might account for some (but not all) of the observed deviations of K_Q from a constant value.

Concluding Remarks

The experiments reported here indicate that the fracture behavior of thin sections containing surface cracks may be strongly influenced by the ratio of the crack-tip plastic zone size to the ligament depth (thickness minus crack depth). The experimental results can be summarized as follows:

1. When the Irwin plastic zone size at fracture was less than about one-tenth of the ligament depth, fracture behavior was in general as predicted by plane-strain theory.

2. When the plastic zone size was greater than the ligament depth, fracture stresses for surface-crack specimens were very nearly the same as for specimens with through cracks of the same original length. It should be recognized that these conclusions may not be applicable to other materials and/or thicknesses, and more definitive tests are required to either confirm or correct them.

Based on analysis using current fracture mechanics theory, as supported but limited by these tests, it can be postulated that:

1. Current fracture mechanics methods can be applied to leak-before-burst problems of thinwalled pressure vessels, but only if the plastic zone at failure is small with respect to the uncracked ligament. If so, leaks can be expected only for somewhat narrow ranges of crack geometry and material properties.

2. If the plastic zone is expected to penetrate the thickness prior to failure, current analytical methods cannot predict whether a vessel will leak or burst at fracture. Under these circumstances, a cracked tensile specimen may not adequately simulate a cracked pressure vessel.

References

1. Brown, W. F., Jr. and Srawley, J. E., Plane Strain Crack Toughness Testing of High Strength Metallic Materials, Spec. Tech. Publ. No. 410, American Society for Testing and Materials, Philadelphia, 1967.

2. Irwin, G. R., Journal of Applied Mechanics, Vol. 29, No. 4, Dec. 1962, pp. 651-654.

3. Anon., "Proposed Method of Test for Plane-Strain Fracture Toughness of Metallic Materials," 1969 Book of ASTM Standards, Part 31, pp. 1099-1114, ASTM, May 1969.

4. Amateau, M. F. and Steigerwald, E. A., "Test Methods for Determining Fracture Toughness of Metallic Materials," Technical Report AFML-TR-67-145, Air Force Materials Laboratory, Dayton, Ohio, Sept. 1967.

5. Srawley, J. E. and Brown, W. F., Jr., in Symposium on Fracture Toughness Testing and its Applications, Spec. Tech. Publ. No. 381, American Society for Testing and Materials, Philadelphia, 1965, pp. 133-198. (Also available as NASA TN D-2599, 1965.)

6. Orange, T. W., "Fracture Toughness of Wide 2014-T6 Aluminum Sheet at -320° F," NASA Report TN D-4017, National Aeronautics and Space Administration, Cleveland, Ohio, 1967.

7. Kuhn, P., Materials Research and Standards, Vol. 8, No. 9, Sept. 1968, pp. 21-26.

8. Rice, J. R., in Symposium on Fatigue Crack Propagation, Spec. Tech. Publ. No. 415, American Society for Testing and Materials, Philadelphia, 1967, pp. 247-311.

9. Hahn, G. T. and Rosenfield, A. R., "Plastic Flow in the Locale on Notches and Cracks in Fe-3Si Steel Under Conditions Approaching Plane Strain," Report SSC-191, Ship Structure Committee, Dept. of the Navy, Nov. 1968.

10. Ayres, D. J., "A Numerical Procedure for Calculating Stress and Deformation Near a Slit in a Three-Dimensional Elastic-Plastic Solid," NASA Report TN D-4717, National Aeronautics and Space Administration, 1968.

11. Kobayashi, A. S. and Moss, W. L., in Fracture; Proceedings of the Second International Conference on Fracture, Chapman and Hall Ltd., 1969, pp. 31-45.

12. Irwin, G. R. and Srawley, J. E., "Progress in the Development of Crack Toughness Fracture Tests," Materialprüfung, Vol. 4, No. 1, Jan. 20, 1962, pp. 1-11.

13. Anderson, R. B. and Sullivan, T. L., "Fracture Mechanics of Through-Cracked Cylindrical Pressure Vessels," NASA Report TN D-3252, National Aeronautics and Space Administration, 1966.

14. Eiber, R. J., Maxey, W. A., Duffy, A. R., and McClure, G. M., "Behavior of Through-Wall and Surface Flaws in Cylindrical Vessels," presented at the National Symposium on Fracture Mechanics, Lehigh Univ., Bethlehem, Pa., June 1968. (To be published in Jour. Engr. Fracture Mech.)

15. Masters, J. N., Haese, W. P., and Finger, R. W., "Investigation of Deep Flaws in Thin Walled Tanks," NASA Report CR-72606, Boeing Company, Dec. 1969.

16. Pyle, R., Schillinger, D. E., and Carman, C. M., "Plane Strain Fracture Toughness and Mechanical Properties of 2219-T87 Aluminum and 5Al-2.5Sn ELI Titanium Alloy Weldments and One Inch Thick 5Al-2.5Sn ELI Titanium Alloy Plate, Report FA-R-1897, NASA Report CR-72154, Frankford Arsenal, Sept. 1968.

17. Hall, L. R., "Plane-Strain Cyclic Flaw Growth in 2014-T62 Aluminum and 6Al-4V (ELI) Titanium," Report DR-114465-1, NASA Report CR-72396, Boeing Co., Nov. 1968.

TABLE 1—Chemical composition of materials tested (percent by weight)

Alloy	Al	C	Cr	Cu	Fe	H	Mg	Mn	N	O	Si	Sn	Ti	V	Zn	Zr
Ti-5Al-2.5 Sn (0.06 in.)	5.3	0.02	----	----	0.18	0.0040	-----	0.01	0.007	0.098	----	2.5	bal.	----	----	----
Ti-5Al-2.5 Sn (0.11 in.)	5.3	0.02	----	----	0.18	0.0034	-----	0.01	0.007	0.091	----	2.5	bal.	----	----	----
Alum. 2014-T6	bal.	----	0.04	4.45	0.60	0.0005	0.57	0.69	0.0012	0.0005	0.92	---	0.02	----	0.05	----
Alum. 2219-T87	bal.	----	----	5.85	0.19	------	0.012	0.25	------	------	0.12	---	0.09	0.08	0.09	0.11

TABLE 2—Tensile properties of test materials (average: longitudinal direction)

Alloy	Test Temperature		Yield Strength		Ultimate Strength		Elastic Modulus		Elongation in 2 in. (5 cm), percent
	deg F	deg K	ksi	MN/m^2	ksi	MN/m^2	psi	N/m^2	
Ti-5Al-2.5 Sn	+70	300	119	821	129	887	17×10^6	120×10^9	14
(0.06-in.)	-320	77	193	1330	202	1390	19	130	16
(1.6-mm)	-423	20	228	1570	247	1710	19	130	13
Ti-5Al-2.5 Sn	+70	300	105	727	114	785	17×10^6	120×10^9	18
(0.11-in.)	-320	77	178	1230	189	1300	19	130	19
(2.9-mm)	-423	20	211	1450	223	1540	(a)	(a)	(a)
Alum. 2014-T6	+70	300	65.0	448	72.3	499	10×10^6	72×10^9	(b)
	-320	77	75.2	519	86.7	598	12	79	(b)
	-423	20	80.3	554	99.7	687	12	80	(b)
Alum. 2219-T87	+70	300	55.0	379	67.7	467	11×10^6	74×10^9	11
	-320	77	64.5	445	84.0	579	11	79	12
	-423	20	70.7	487	96.3	664	12	83	14

[a]Measurement considered unreliable.

[b]Not measured.

TABLE 3—Through-crack fracture test data

Alloy	Test Temperature		Specimen Width, W		Specimen Thickness, t		Initial Crack Length, 2c		Gross Fracture Stress, σ		Nominal Fracture Toughness, K_{cn}	
	deg F	deg K	in.	mm	in.	mm	in.	mm	ksi	MN/m^2	$ksi\sqrt{in.}$	$MNm^{-3/2}$
Ti-5Al-2.5 Sn	-423	20	2.00	51	0.0624	1.58	0.080	2.0	147.1	1010	58.7	64.5
			1.00	25	.0616	1.56	.085	2.2	131.1	904	52.8	58.0
			2.00	51	.0632	1.61	.141	3.6	123.0	848	62.9	69.1
			1.00	25	.0639	1.62	.172	4.4	115.5	796	66.2	72.7
			2.00	51	.0632	1.61	.179	4.5	115.1	794	65.8	72.3
			1.00	25	.0629	1.60	.414	10.5	63.9	441	60.1	66.0
			2.00	51	.0640	1.63	.420	10.7	78.3	540	67.8	74.5
			1.00	25	.0640	1.83	.481	12.2	54.6	376	57.7	63.4
			2.00	51	.0628	1.60	.793	20.1	46.8	323	59.1	64.9
			3.00	76	.0640	1.63	.988	25.1	48.5	334	66.0	72.5
			3.00	76	.0639	1.62	.995	25.3	44.9	310	61.2	67.2
Ti-5Al-2.5 Sn	-423	20	1.00	25	0.1115	2.83	0.123	3.1	161.3	1110	86.7	95.3
			2.00	51	.1122	2.85	.129	3.3	158.3	1090	84.6	93.0
			1.00	25	.1126	2.86	.240	6.1	116.9	806	83.1	91.3
			2.00	51	.1135	2.88	.269	6.8	119.0	821	86.0	94.5
			1.00	25	.1128	2.87	.360	9.1	90.3	623	80.4	88.3
			2.00	51	.1128	2.87	.381	9.7	97.3	671	82.3	90.4
			3.00	76	.1162	2.95	.994	25.2	58.3	402	80.5	88.5
			3.00	76	.1157	2.94	1.051	26.7	55.2	381	79.1	86.9
Alum. 2014-T6	-423	20	3.00	76	0.0613	1.56	0.277	7.0	59.3	409	46.5	51.1
					.0622	1.58	.278	7.1	58.8	405	46.0	50.5
					.0617	1.57	.557	14.1	46.5	321	49.6	54.5
					.0600	1.52	.775	19.7	41.9	289	53.3	58.6
					.0613	1.56	.846	21.5	39.5	272	52.6	57.8
					.0611	1.55	1.032	26.2	34.2	236	50.9	55.9
					.0604	1.53	1.187	30.1	32.2	222	53.0	58.2
					.0602	1.53	1.204	30.6	31.5	217	52.2	57.4
					.0608	1.54	1.399	35.5	28.4	196	53.0	58.2
					.0611	1.55	1.432	36.4	27.5	190	52.2	57.4
Alum. 2219-T87	+70	300	5.5	140	0.0676	1.72	0.334	8.5	52.5	362	53.1	58.3
					.0672	1.71	.402	10.2	51.3	354	56.1	61.6
					.0673	1.71	.515	13.1	49.8	343	60.8	66.8
					.0676	1.72	.623	15.8	47.9	330	63.2	69.4
			6.7	170	.0670	1.70	.909	23.1	47.3	326	76.0	83.5
					.0680	1.73	1.004	25.5	46.1	318	77.1	84.7
					.0682	1.73	1.186	30.1	43.4	299	77.5	85.2
	-320	77	5.5	140	.0685	1.74	.332	8.4	63.2	438	64.9	71.3
					.0687	1.74	.420	10.7	61.5	424	69.6	76.5
					.0680	1.73	.480	12.2	60.2	415	72.1	79.2
					.0676	1.72	.621	15.8	57.1	394	75.5	83.0
			6.7	170	.0673	1.71	.884	22.5	55.9	385	88.1	96.8
			6.7	170	.0883	1.73	.998	25.3	54.6	376	90.9	99.9
			6.7	170	.0686	1.74	1.203	30.6	51.1	352	91.7	100.8
	-423	20	5.5	140	.0682	1.73	.297	7.5	66.7	460	61.3	67.4
					.0680	1.73	.400	10.2	64.6	445	67.7	74.4
					.0672	1.71	.492	12.5	62.6	432	71.5	78.6
					.0675	1.71	.610	15.5	61.5	424	78.2	85.9
			6.7	170	.0683	1.73	.825	21.0	58.2	401	83.9	92.2
					.0676	1.72	.891	22.6	57.5	396	85.9	94.4
					.0686	1.74	1.027	26.1	55.7	384	88.9	97.7
					.0684	1.74	1.184	30.1	53.6	370	91.4	100.4

TABLE 4—Surface-crack fracture test data

Alloy	Test Temperature		Specimen Width, W		Specimen Thickness, t,		Crack Depth, a		Crack Length, 2c		Gross Fracture Stress, σ		Apparent Fracture Toughness, K_Q	
	deg F	deg K	in.	mm	in.	mm	in.	mm	in.	mm	ksi	MN/m^2	ksi $\sqrt{in.}$	$MNm^{-3/2}$
Ti-5Al-2.5 Sn (0.06-in.) (1.6-mm)	-423	20	1.00	25	0.0630	1.60	0.022	0.56	0.089	2.26	207.6	1430	51.8	56.9
			1.00	25	.0628	1.60	.024	.61	.078	1.98	207.5	1430	49.8	54.7
			1.00	25	.0631	1.60	.027	.69	.065	1.65	213.3	1470	47.1	51.8
			2.00	51	.0635	1.61	.027	.69	075	1.91	182.7	1260	42.8	47.0
			1.00	25	.0636	1.62	.031	.79	.077	1.96	180.8	1250	43.1	47.4
			2.00	51	.0643	1.63	.033	.84	.099	2.51	169.0	1170	45.4	49.9
			2.00	51	.0621	1.58	.034	.86	.132	3.35	152.3	1050	46.0	50.5
			1.00	25	.0648	1.65	.037	.94	.102	2.59	153.5	1060	42.0	46.1
			2.00	51	.0635	1.61	.038	.97	.122	3.10	152.0	1050	45.3	49.8
			1.00	25	.0647	1.64	.040	1.02	.123	3.12	137.9	951	41.3	45.4
			2.00	51	.0641	1.63	.040	1.02	.128	3.25	145.7	1000	44.6	49.0
			1.00	25	.0650	1.65	.041	1.04	.147	3.73	130.0	896	42.1	46.3
			2.00	51	.0628	1.60	.046	1.17	.158	4.01	107.4	741	37.1	40.8
			1.00	25	.0640	1.63	.050	1.27	.173	4.39	102.4	706	37.9	41.6
			2.00	51	.0646	1.64	.051	1.30	.175	4.45	98.0	676	36.6	40.2
			2.00	51	.0646	1.64	.056	1.42	.190	4.83	96.7	667	40.2	44.2
			1.00	25	.0642	1.63	.056	1.42	.200	5.08	101.5	700	43.8	48.1
			2.00	51	.0631	1.60	.031	.79	.297	7.54	138.3	954	48.2	53.0
			1.00	25	.0630	1.60	.033	.84	.286	7.26	136.9	944	48.8	53.6
			1.00	25	.0639	1.62	.033	.84	.300	7.62	136.9	944	49.0	53.8
			1.00	25	.0640	1.63	.034	.86	.391	9.93	143.6	990	54.2	59.6
			2.00	51	.0637	1.62	.035	.89	.399	10.13	138.0	952	52.9	58.1
			1.00	25	.0622	1.58	.037	.94	.393	9.98	120.4	830	47.3	52.0
			2.00	51	.0639	1.62	.043	1.09	.590	14.99	111.7	770	50.0	54.9
			2.00	51	.0633	1.61	.045	1.14	.351	8.92	106.1	732	45.6	50.1
			2.00	51	.0638	1.62	.048	1.22	.782	19.86	85.1	587	42.4	46.6
			2.00	51	.0627	1.59	.049	1.24	.820	20.83	80.6	556	41.5	45.6
Ti-5Al-2.5 Sn (0.11-in.) (2.9-mm)	-423	20	1.00	25	0.1157	2.94	0.023	0.58	0.118	3.00	207.6	1430	56.9	62.5
			2.00	51	.1122	2.85	.037	.94	.129	3.28	195.5	1350	59.8	65.7
			1.00	25	.1133	2.88	.043	1.09	.153	3.89	184.9	1270	61.3	67.4
			1.00	25	.1129	2.87	.056	1.42	.179	4.55	162.1	1120	58.4	64.2
			1.00	25	.1128	2.87	.068	1.73	.227	5.77	144.0	993	58.6	64.4
			2.00	51	.1147	2.91	.073	1.85	.247	6.27	139.9	965	59.6	65.5
			1.00	25	.1111	2.82	.077	1.96	.290	7.37	118.9	820	54.8	60.2
			2.00	51	.1143	2.90	.084	2.13	.291	7.39	129.0	889	61.2	67.2
			1.00	25	.1161	2.95	.097	2.46	.342	8.69	105.4	727	57.1	62.7
			2.00	51	.1119	2.84	.101	2.57	.337	8.56	110.4	761	65.3	71.8
Alum. 2014-T6	-423	20	3.00	76	0.0622	1.58	0.034	0.86	0.206	5.23	72.1	497	25.7	28.2
			2.99	76	.0620	1.57	.035	.89	.213	5.41	70.8	488	25.6	28.1
			2.99	76	.0615	1.56	.038	.97	.311	7.90	63.4	437	25.4	27.9
			2.99	76	.0615	1.56	.042	1.07	.403	10.24	55.1	380	24.1	26.5
			3.01	76	.0600	1.52	.044	1.12	.232	5.89	66.2	456	27.4	30.1
			3.00	76	.0613	1.56	.044	1.12	.265	6.73	63.1	435	26.8	29.4
			2.99	76	.0605	1.54	.046	1.17	.457	11.61	51.7	356	24.7	27.1
			2.99	76	.0612	1.55	.051	1.30	.609	15.47	47.8	330	26.6	29.2
			3.00	76	.0603	1.53	.054	1.37	1.275	32.39	31.4	217	21.5	23.6
			3.01	76	.0600	1.52	.055	1.40	1.115	28.32	33.6	232	24.9	27.4
			3.00	76	.0603	1.53	.055	1.40	1.363	34.62	29.6	204	21.7	23.8
			3.00	76	.0619	1.57	.058	1.47	.198	5.03	66.7	460	34.2	37.6

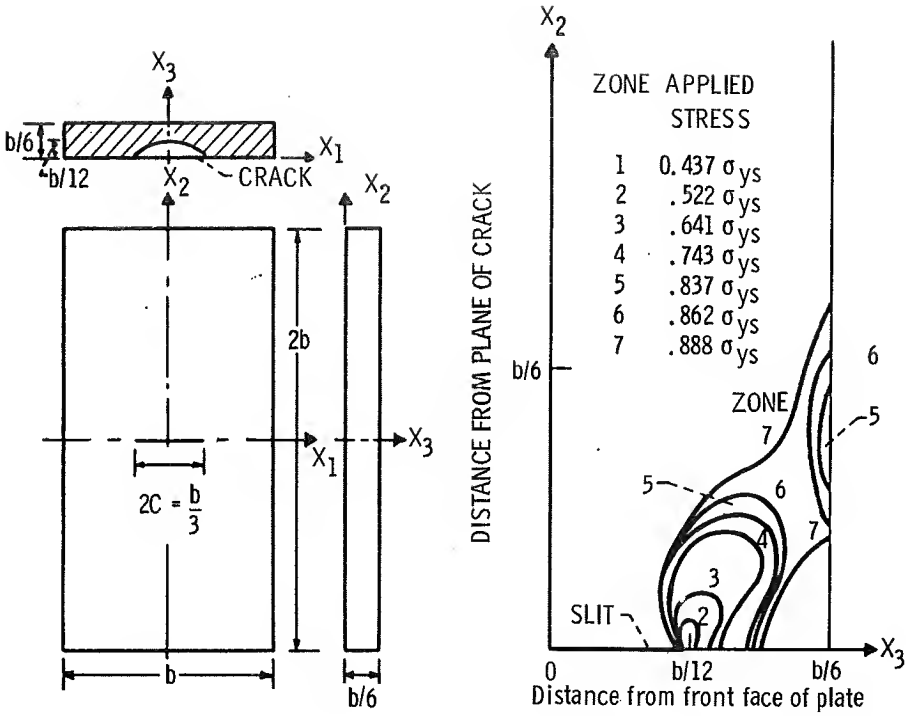

Fig. 1 - Sample plastic zone (ref. 10).

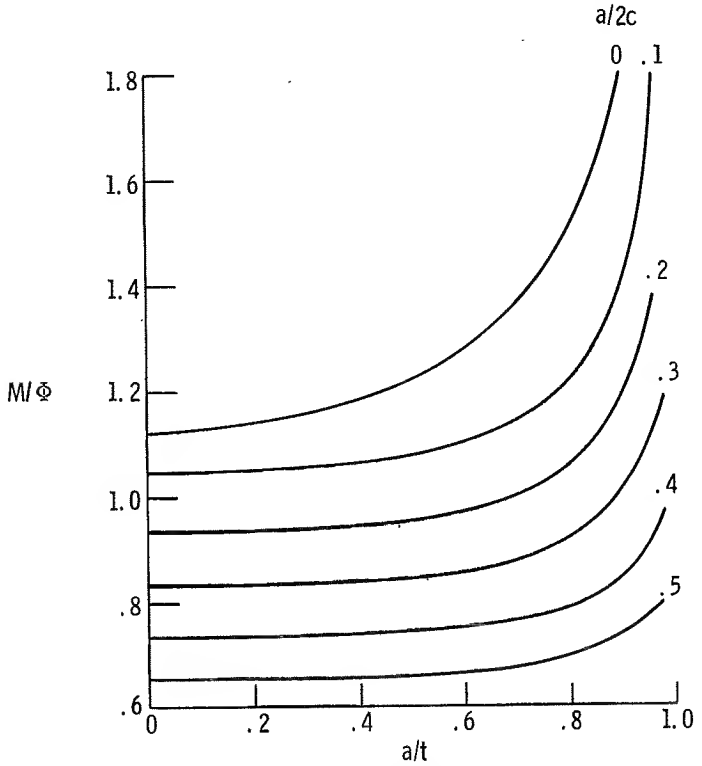

Fig. 2 - Correction factor used in Eq. (2b).

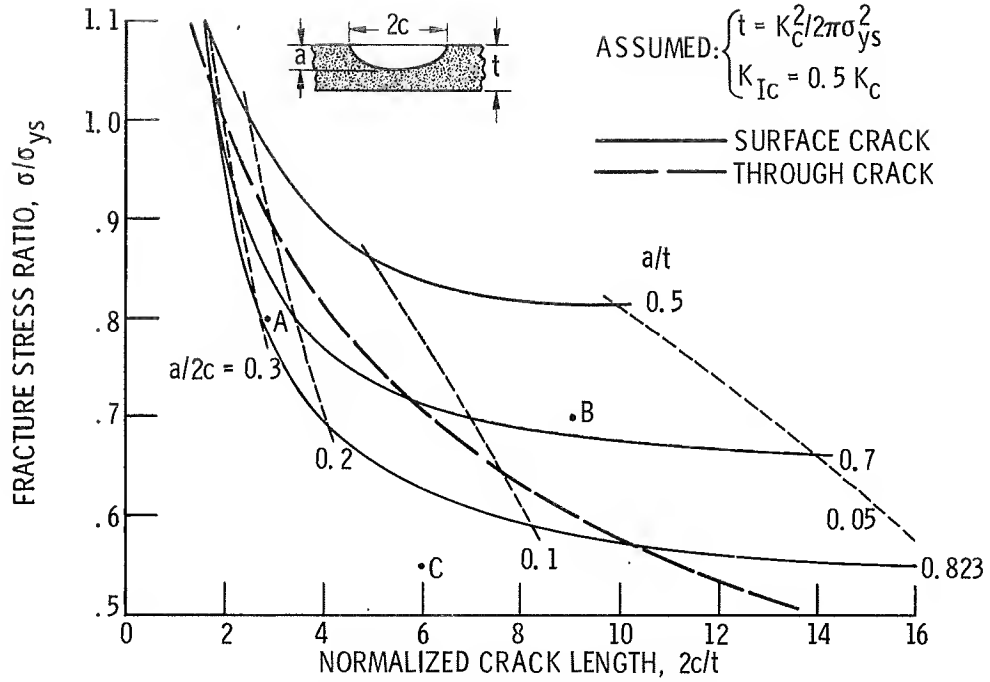

Fig. 3 - Effect of crack geometry on predicted fracture stress for through and part-through cracks.

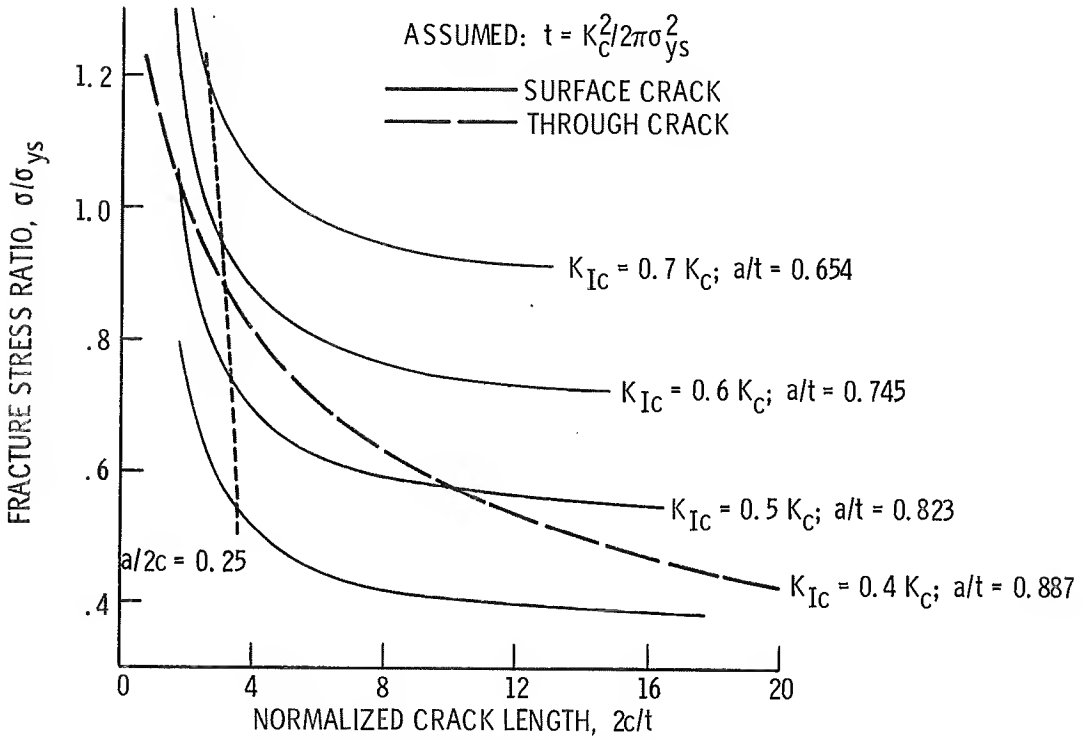

Fig. 4 - Effect of material toughness on predicted fracture stress for through cracks and for part-through cracks at limiting depth.

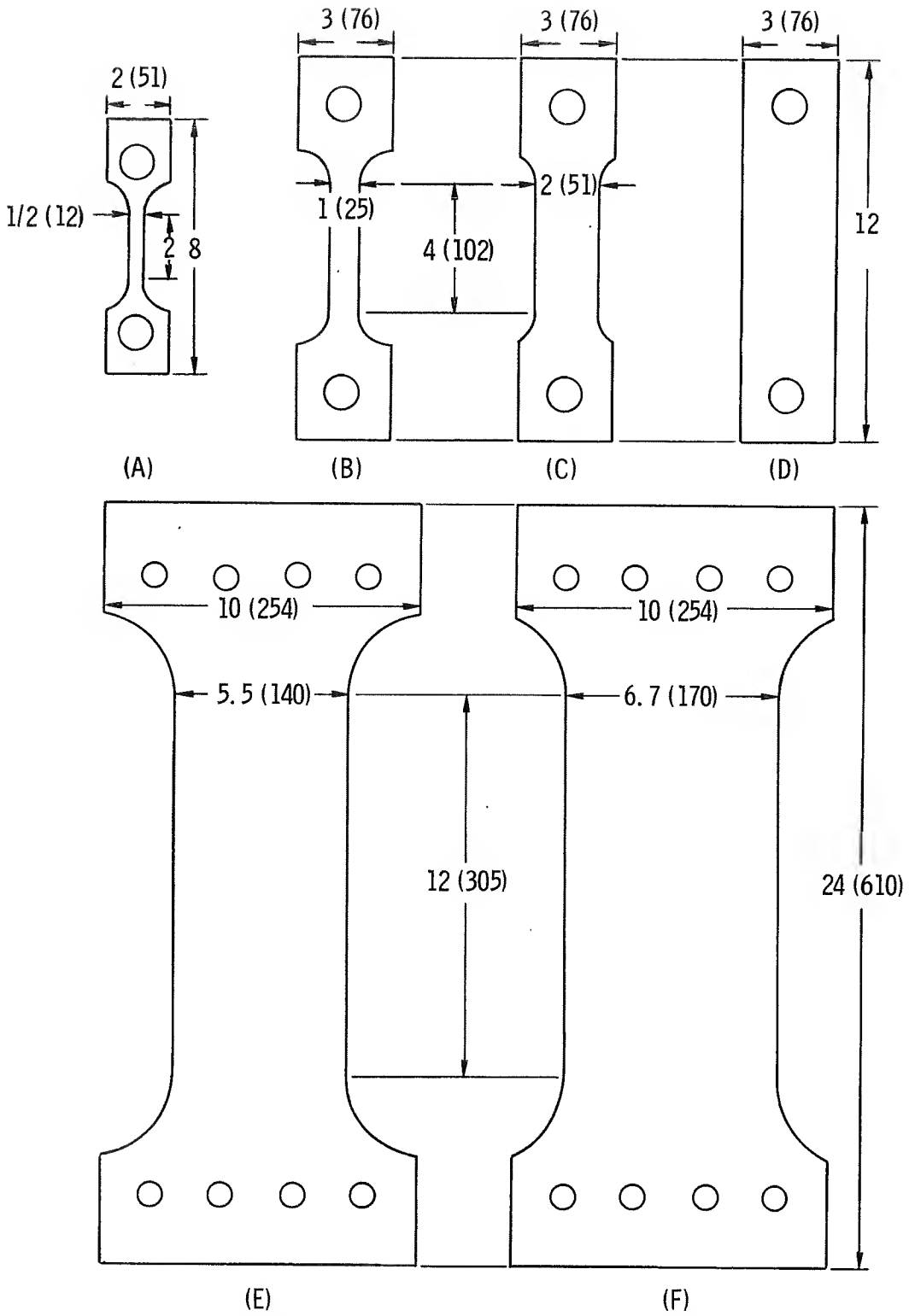

Fig. 5 - Smooth tensile and fracture specimens (dimensions in inches or (mm)).

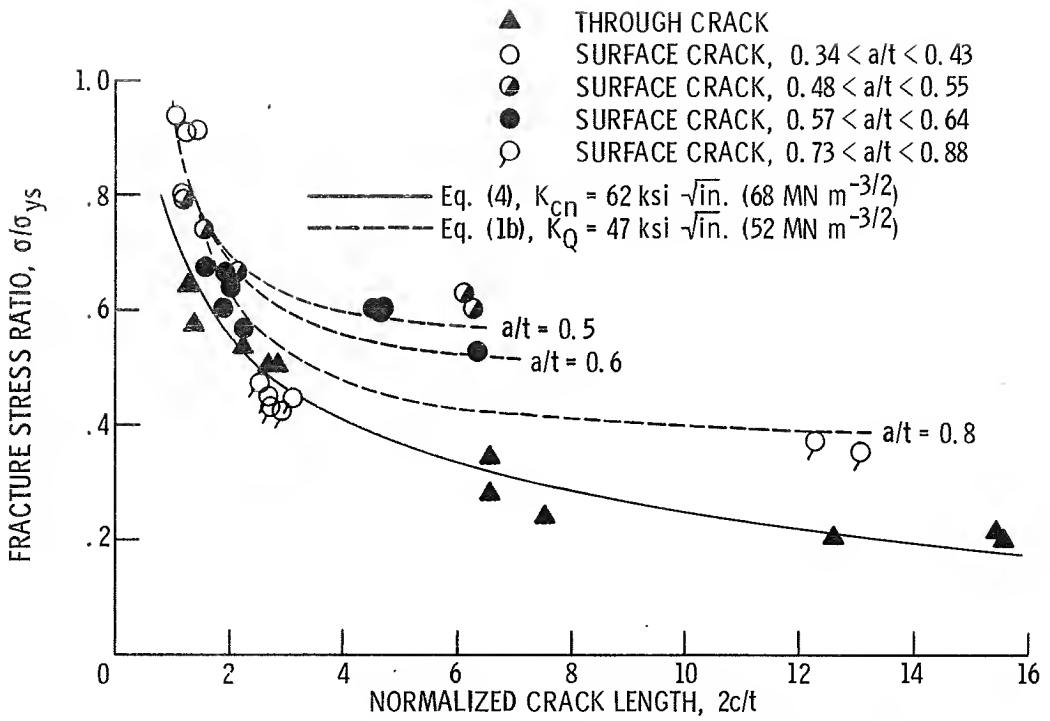

Fig. 6 - Fracture stress for titanium-5Al-2.5Sn-ELI specimens 0.06-inch (1.6-mm) thick (-423° F (20 K); yield strength, 228.0 ksi (1570 MN/m^2)).

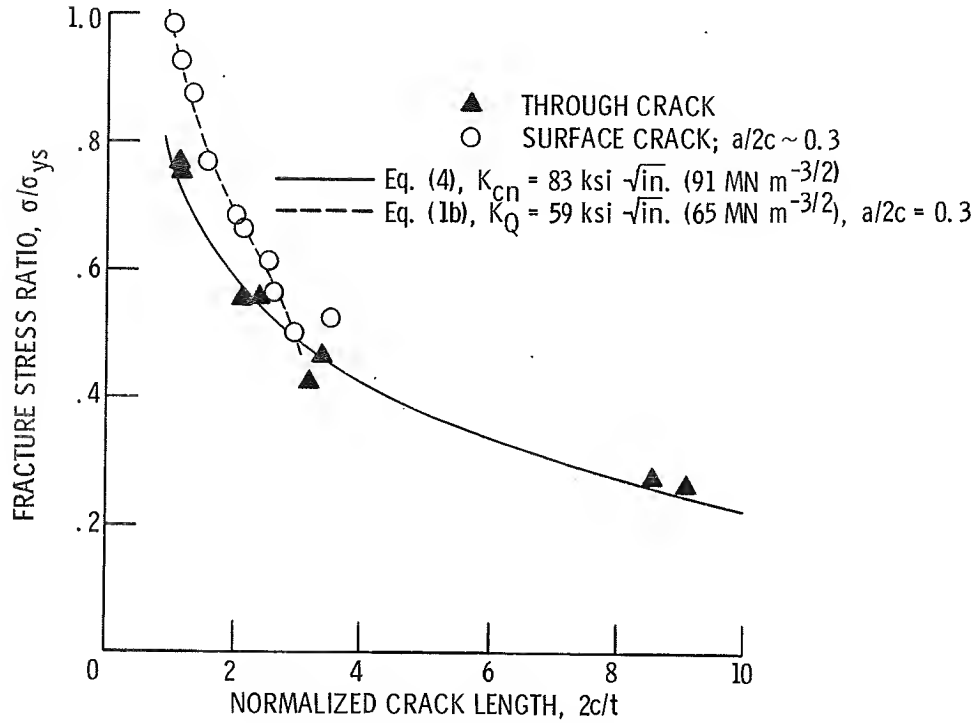

Fig. 7 - Fracture stress for titanium-5Al-2.5 Sn-ELI specimens 0.11-inch (2.9-mm) thick (-423° F (20 K); yield strength, 211 ksi (1450 MN/m^2)).

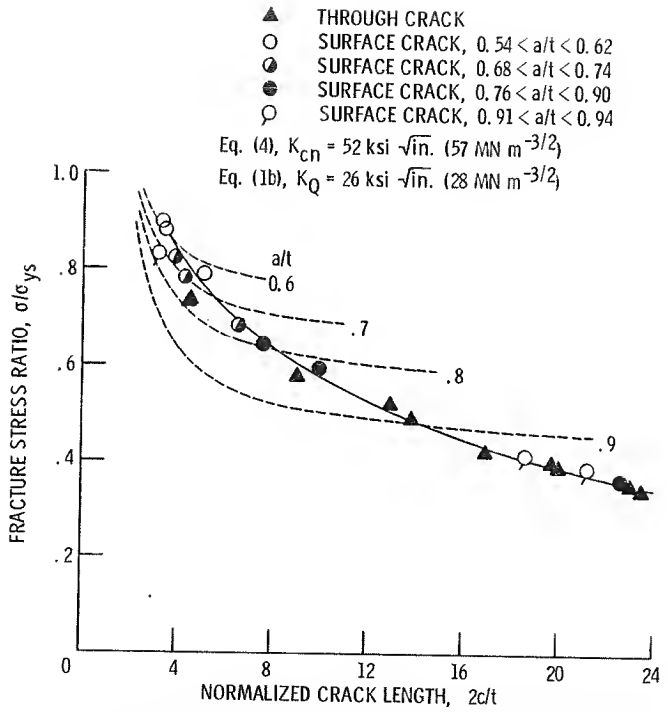

Fig. 8 - Fracture stress for 2014-T6 aluminum specimens (0.06-inch (1.6-mm) thick; -423° F (20 K); yield strength, 80.3 ksi (554 MN/m^2)).

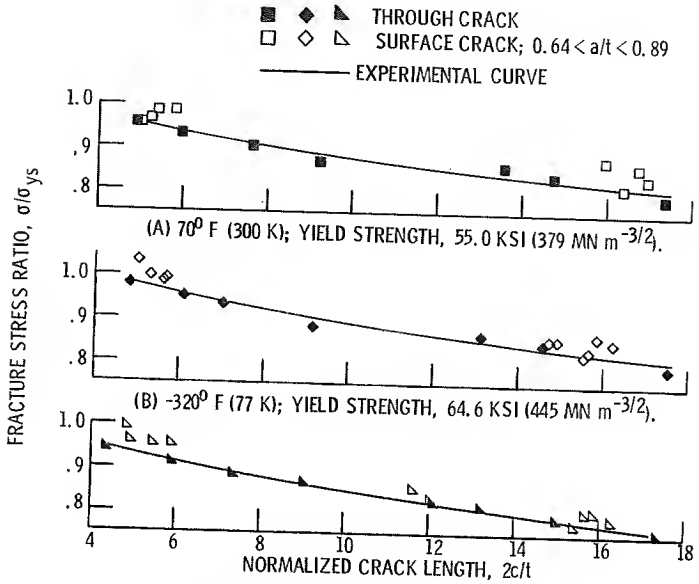

(C) -423° F (20 K); YIELD STRENGTH, 70.8 KSI (487 MN $m^{-3/2}$).

Fig. 9 - Fracture stress for 2219-T87 aluminum specimens (0.07-inch (1.7-mm) thick; surface crack data from ref. 15).